AIAA 81-4255

Hydrodynamics of Podded Ship Propulsion

Dean A. Rains,* David J. VanLandingham,† and Herman C. Schlappi‡
Ingalls Shipbuilding/Litton Industries, Pascagoula, Miss.
Chi Chao Hsiung§
Memorial University of Newfoundland, St. John's, Newfoundland, Canada
and
Karl L. Kirkman¶
Hydronautics, Inc., Laurel, Md.

With the advent of compact high-powered electric motors, it is possible to propel ships with podded propulsion units mounted externally on the ship hull. Propulsion pods may permit quieter propulsion and reduce construction and replacement efforts. This paper explores the value of the pod concept for destroyer application, describes the design features for such application, and examines the hydrodynamics of pods themselves. Drag and performance estimates are made and compared to model-scale test results. Some conclusions are drawn and recommendations are made for future work in this area.

Introduction

A U.S. NAVY/industry team is developing several types of electric ship-drive motors with significantly less diameter, volume, and weight than conventional machinery. Table 1 compares the projected characteristics of several types of advanced motors. The anticipated achievement of the motor's attractive weights and dimensions points to the possibility of close-coupling of the drive motor to the propulsor in a podded unit mounted externally on the hull. Shafting would be minimized in such an arrangement and the volume used for hull machinery would be limited to gas turbine generators and supporting auxiliary spaces. For greater accessibility and minimum interference from the combat system functions, the prime mover/generators can be located conveniently topside. One possible destroyer application of a podded arrangement is shown in Fig. 1. The advantages and disadvantages of the pod concept are listed in Table 2.

The purpose of this paper is to explore the external hydrodynamics of pods to determine their effect on ship drag and performance. The merits of pods are explored by rigorous tradeoff analysis, drag and performance estimates are developed, and model tests are used to verify the estimates of drag and propulsive efficiency. The hydrodynamics of performance is an important parameter in the decision-making process to determine the utility of the pod concept.

Value of Podded Propulsion—Rationale for Interest

There are many possible advantages of podded propulsion (see Table 2). Appendage drag may be reduced not only by replacing long open shafts and multiple struts with pods and single struts, but by integrating the rudder into the pod/strut body and eliminating bilge keels and skeg. With the propeller oriented to a tractor configuration, the rudder can be integrated into the trailing edge of the pod/strut body as shown in Fig. 1. With the large positive directional stability of pods and struts, the skeg can be eliminated, and the large rolling moment of pods and struts allows removal of the bilge keels. Dry-docking is not affected because the propeller extends below the ship baseline the same distance as in a conventional installation.

Results of a performance analysis of the configuration in Fig. 1 are plotted in Fig. 2. Because of the use of pods compared to conventional open shafts, horsepower changes are estimated for the same DD-963 class hull. Bilge keels and skeg are removed for the podded arrangement and the rudders are integrated into the pod/strut bodies. The rudders are the same size in both cases.

The removal of long shafting, bearings, and reduction gears reduces the hull volume required for podded propulsion machinery. Using the flexibility inherent in electric drive motors, propulsion plant volume in the hull can be further reduced by moving the prime movers higher in the ship, thus, eliminating some or all of the straight ducting needed for the intakes and exhausts. This same advantage can be utilized in conventional inboard electric drives. Because of these reductions in propulsion plant volume, more payload can be added or the hull size can be reduced. Reducing hull size lowers construction costs and hull drag.

Estimated efficiencies and specific powerplant weights and volumes for pods and several other propulsors were applied in a computerized tradeoff study using a ship size and design program at Ingalls.[1] This design program was used to evaluate the impact on ship size and fuel load for each of the propulsion plants when each supports the same payload (635 long tons and 204,500 ft^3), top speed (32.5 knots) and endurance (6000 n.mi.).

The fuel load required to carry the fixed payload at cruise speed for the specified endurance period was used to measure the relative energy consumption of the various power plants. Table 3 lists the results of the analysis as percentage changes from the baseline. The displacements and fuel loads are also indicated in each case, with the pod drag factored into these performance calculations. The potential savings shown by trail shaft (one unpowered shaft) is based on analytical evaluation and further study is recommended in this area.

The conclusion of this parametric ship design study is that cross-connecting machinery (operating the ship at cruise speed with two propellers, but with only one of the two turbines) improves propulsion plant efficiency. Because of a unique characteristic, gas turbines drop off rapidly in performance as the load is reduced. Powerplant weight and volume reductions combine with this performance improvement to greatly improve the ship (24.8% reduction in fuel load and 16.6% reduction in ship displacement) over the baseline configuration.

Received Aug. 7, 1980; revision received April 15, 1981.

*Director, Advanced Programs; presently, Principal Scientist, Ramcor, Inc. Member AIAA.

†Senior Engineer.

‡Senior Engineer.

§Associate Professor, Engineering and Applied Science

¶Engineer.

A more detailed design study was conducted to compare ship size, arrangement, volume, and damage control features of a podded, electrically driven ship to one with the same electric drive machinery (super conductive homopolar) in a conventional inboard arrangement with the gas turbine/ generators located down in the engine rooms on a computer-synthesized "general purpose destroyer" design.[1,2] The design study included development of ship arrangements (inboard profile and deck plans), for the podded ship. The rudder on the pods was sized to give the same turning radius as that of a ship with open shafts (1063 ft at 30 knots and 35-deg rudder angle).

The results of this ship-sizing study are listed in Table 4. Other ship-characteristic comparisons were made at 20 knots and they are listed in Table 5. All of the study results indicated that a podded destroyer has significant advantages in ship size, performance, and fuel consumption, compared to a destroyer with the same machinery in a conventional arrangement.

These layouts demonstrate one of the principal advantages of the podded arrangement: the powerplant is compact and conveniently located near the stern so most of the hull can be devoted to payload functions and crew compartments without interference.

Table 1 Projected characteristics of electric drive motors 40,000 hp at 2.8 R/S

Motor concept	Weight, long tons	Length, ft	Diameter, ft	Efficiency, %, Maximum power	Efficiency, %, Cruise power
Superconducting acyclic dc	41	12.1	6.4	97.5	98.5
Normal conducting acyclic dc (oil cooled)	59	11.5	7.9	97.7	97.5
Normal conducting SEGMAC dc (water cooled)	54	9.3	10.6	97.0	96.3

Table 2 Advantages and disadvantages of podded electric drive compared to conventional electric drives

Advantages	Disadvantages
Reduced machinery space required in hull	Increased drag due to pods as motor diameter increases
Main machinery is accessible for removal and replacement as pods	Drive motor is more exposed to damage
A tractor propeller can be used to maximize cavitation-free forward speed (no wake variations in inflow to propeller)	Increased ship turning radius due to fin effect of pod/strut
Convenient arrangement possible to avoid interference with topside payload functions	The main drives are less accessible from inside the hull

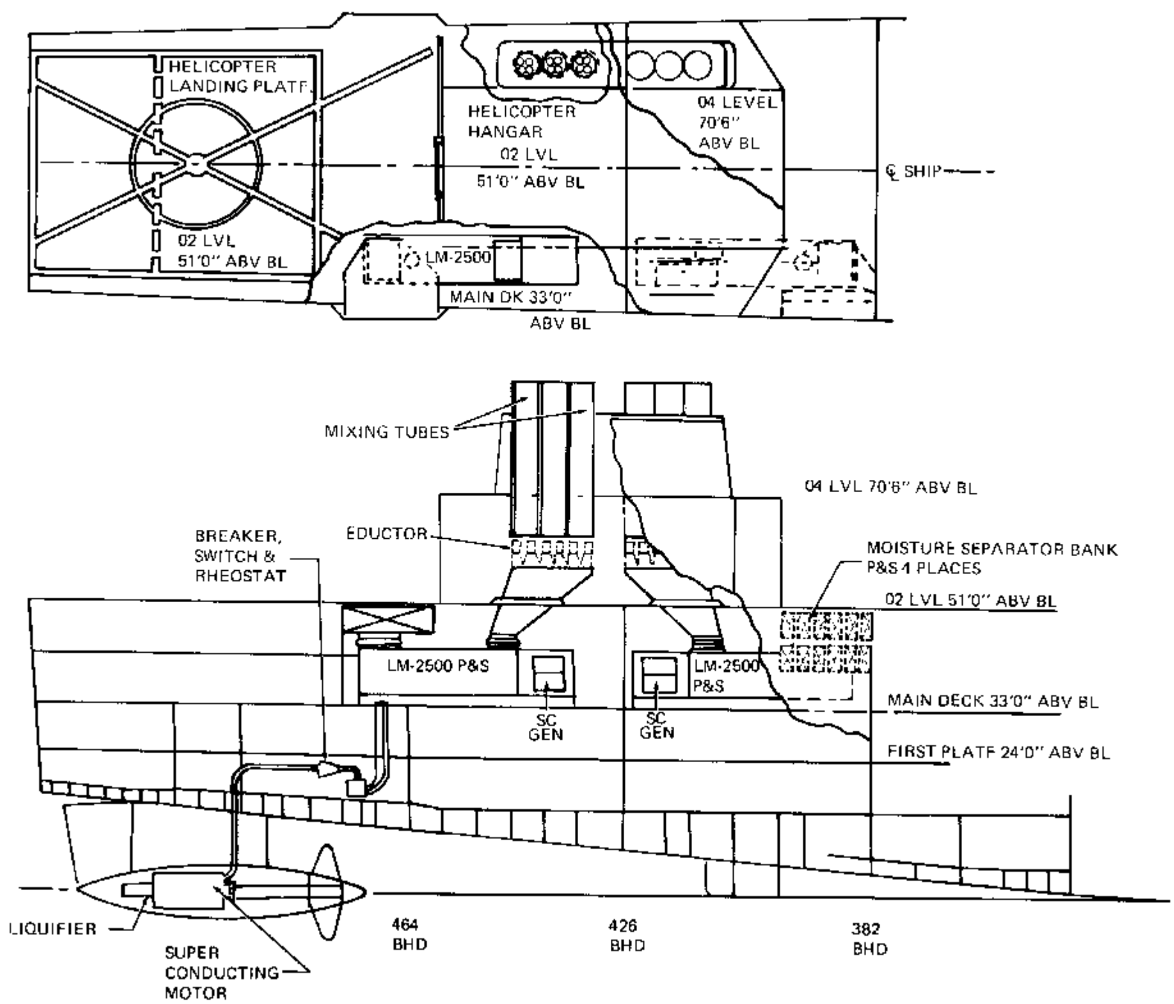

Fig. 1 Podded d.c. superconducting electric drive for application to a DD-963 class hull.

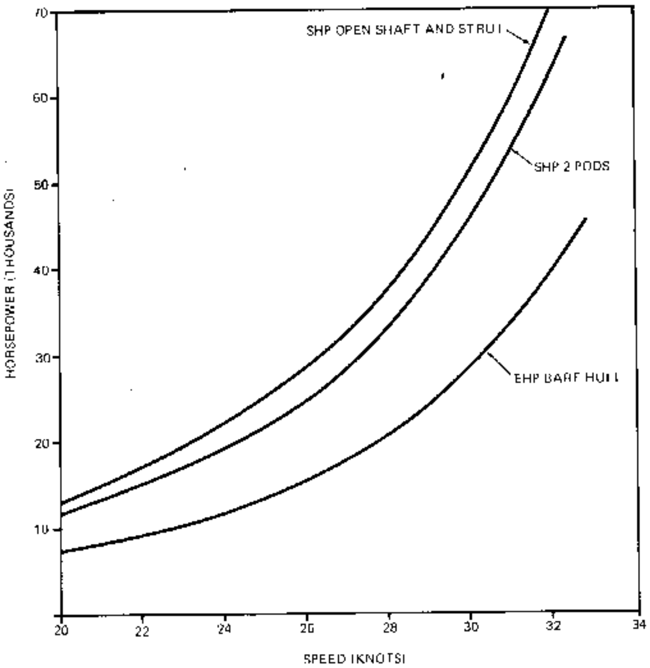

Fig. 2 Shaft horsepower comparison at constant hull and rudder size.

Table 3 Comparison of ship size and fuel load of conventional mechanical powerplants vs pod electric powerplant in large destroyers

	Configuration	Displacement, long tons	Fuel load, long tons	
1	Two 17-ft-diam CRP propellers Mechanical drive	7892 0	1615 0	Baseline
2	Two 17-ft-diam CRP propellers Trail shaft	7315 −7.3	1357 −16.0	% change
3	Two 24-ft-diam overlapping CRP propellers Mechanical drives	8083 +2.4	1575 −2.5	% change
4	Two 17-ft-diam fixed-pitch propellers Pod electric drives	6580 −16.6	1214 −24.8	% change

In addition to reducing energy consumption, one of the most attractive features of podded propulsion is its potential for quietness. By using electric drive, gear noise is eliminated. Reversal is achieved electrically with switchgear, enabling fixed-pitch propellers to be used and eliminating the hydraulics noise and larger hub associated with controllable reversible-pitch propellers. The direct-current homopolar motors now in development will be even quieter than alternating current machines because they do not have any large alternating magnetic fields. The largest source of underwater radiated noise is generally propeller cavitation, and with podded propulsors the propeller can easily be oriented to a tractor configuration. With no leading appendages, flow to a tractor propeller is far more uniform than it is with a pusher pod or conventional open shafts. With the more uniform flow, the tractor propeller is less likely to cavitate at high speeds.

Installation and replacement of pods can be quicker and simpler than with conventional shafting. The pod can be fabricated and tested in a shop and installed as a module; whereas conventional shafting requires numerous alignments of individual components inside the hull. While shaft seals are required for each of the bulkhead and hull penetrations in conventional shafting, a podded propulsor requires only the gland seal in the pod.

Table 4 Results of the comparison of conventional vs podded electrical drive for a medium-sized destroyer

	Open-shaft	Podded	Change, %
Full-load displacement, long tons	6399	5412	−15
Total enclosed volume, ft^3	813,122	692,667	−15
Endurance fuel rate, lb/h	5755	4616	20
Length (between perpendiculars), ft	472	452	−4
Beam, ft	55	50	−9
Draft, ft	17.3	16.3	−6

Table 5 Performance comparison conventional vs podded medium-sized destroyer (both with superconducting dc drive motors)

	Open-shaft	Podded
20 Knots		
Propeller rpm	90	83
Propulsive coefficient	0.72	0.74
SHP	11,990	8072
SFC, lb/hp-h	0.48	0.57
Fuel load	964	810
30 Knots		
Head reach, ft	980	1012
Stopping time, s	43.1	44.5
Turning radius at at 35-deg rudder angle, ft	1063	1063

There are some disadvantages of podded propulsion. The drive motor is more exposed to catastrophic loss in the podded arrangement than it is in the engine room; it is also much less accessible in the pod, so maintenance is more difficult. The large positive directional stability of pods and struts means that either the turning radius will be greater or the rudder will be larger than with conventional methods.

Computation for Predicting Pod/Strut Drag

The resistance of the pod-strut system is predicted using methods outlined in Hoerner's *Fluid Dynamic Drag.*[3] The drag coefficient of the pod, based on its surface area, is

$$C_D = C_f[1 + 1.5(d/L)^{1.5} + 7(d/L)^3]$$

where d/L is the diameter-length ratio of the pod. The drag coefficient of the strut, based on planform area is

$$C_D = 2C_f[1 + 2(t/c) + 60(t/c)^4]$$

where t/c is the thickness-chord ratio of the strut. C_f is the skin friction surface drag coefficient. The drag coefficient for intersection of the strut with nacelle or hull is

$$C_D = (\mathrm{FF})[17(t/c)^2 - 0.05]$$

where C_D is based on the thickness squared and FF is the fillet factor, which is taken to be 0.20 from Ref. 3 (Fig. 26, p. 8-11). The proximity drag coefficient is based on the diameter of the body of revolution squared.

Proximity drag is considered for two cases: pod-to-pod interference and pod-to-hull interference. Strut-to-strut interference is negligible because of the thinness of the struts considered. The ratio of separation-to-thickness for the struts is 6.08 in the model test configuration. Reference 3 (Fig. 6, p. 8-3) shows no increase in drag coefficient for ratios this large.

For pod-to-pod proximity, the ratio of pod separation to pod diameter is 1.68 which would increase C_D by 0.05 above the level for friction drag in Ref. 3 (Fig. 6, p. 8-3). However,

Table 6 Mean wake fractions and jet velocities (used in algorithm to predict model-test results)

Element	Distance from hull, ft Minimum	Maximum	Mean wake fraction (w)	$1-W$ or (V_j'/V_s)
Tractor pods				
1 in. fillet at hull	0	0.08	0.9197	0.0803
Propeller	3.50	20.50	0.0541	0.9459
Strut in hull wake	0	5.05	0.3626	0.6374
Strut in prop jet	5.05	8.73	...	1.0060
1 in. fillet at pod	8.65	8.73	...	1.0060
Pod in prop jet	8.73	18.23	...	1.0060
Pod proximity	8.73	18.23	0.0148	0.9852
Pusher pods				
1 in. fillet at hull	0	0.08	0.9197	0.0803
Strut	0	7.75	0.2834	0.7166
1 in. fillet at pod	7.67	7.75	0.0980	0.9020
Pod	7.75	17.25	0.0236	0.9764

Table 7 Model-test dimensions used in computation (in full-scale feet: 2.07 ft/in.)

	Tractor pods	Pusher pods
Propeller top-to-hull clearance	3.50	5.54
Pod diameter (maximum)	9.50	9.50
Pod overall length	52.15	50.50
Strut thickness (maximum)	3.60	3.60
Strut chord length	24.00	24.00
Strut height (at apex of pod curvature)	8.73	7.75
Pod separation (center-to-center)	25.50	25.50

that figure is a plot of C_D for adjacent struts with parallel sides. The pods are not constant in separation since their adjacent sides are curved in two dimensions instead of one. Mean thickness t at maximum pod diameter d is $\pi/4\ d$. The mean separation s to thickness ratio is $(x-t)/t$ where x is the center-to-center separation of the pods. The drag coefficient for pod-to-pod proximity is approximated by

$$C_D=(0.155)\exp[-(s/t-0.25)^{1.1}/1.1]$$

based on projected area.

For pod-to-hull proximity, the ratio of separation y to pod diameter d is used to estimate the drag coefficient based on projected area

$$C_D=(0.0642)(y/d)^{-5.7818}$$

Originally developed to facilitate tradeoff studies of wake induction, a model for the wake profile in the propulsor vicinity is included in the pod/strut drag computation. Based on early, unclassified model tests of a modern destroyer hull, the advance ratio V_A/V_S varies in magnitude with the distance y from the hull. V_A is the local advance velocity and V_S is ship velocity. Taken along a vertical line through the center of the propeller disk, the magnitude of V_A/V_S is approximated by the function $f(y)=0.5009+0.45\ \log_{10}(y+0.07706)$ out to 12.75 ft from the hull, and $f(y)=1.0$ beyond 12.75 ft.

Averaged across a given structural element from minimum (y_{min}) to maximum (y_{max}) distance from the hull, the mean wake fraction w is

$$w=1-\frac{V_A}{V_S}=1-\frac{1}{y_{max}-y_{min}}\int_{y_{min}}^{y_{max}} f(y)\,dy$$

For the portion of the interval $(y_{max}-y_{min})$ that is 12.75 ft or closer from the hull,

Table 8 DD-963 class ship and model particulars

	Ship	Model
Length (water line), ft	530.0	21.34
Length (between perpendiculars), ft	529.0	21.30
Beam (mid-length), ft	55.0	2.21
Draft (mid-length), ft	19.5	0.76
Displacement	8000.0 long tons (fresh water)	1136.7 lb (salt water)
Wetted surface (appended), ft^2		
No propulsion appendages	33,696	54.61
Standard propulsion appendages	35,411	57.39
Tractor pods	36,534	59.21
Pusher pods	36,405	59.00
Trim, ft	0	0
C_B	0.461	0.461
C_P	0.560	0.560
C_x	0.823	0.823
L/B_x	9.62	9.62
Propeller diameter (twin screw), ft	17.0	0.684
Linear scale ratio	1.0	24.84

$$\int_{y_{min}}^{\alpha} f(y)\,dy=0.5009\beta-\frac{0.45}{\ln 10}(\beta)$$

$$+\frac{0.45}{\ln 10}(\alpha+0.07706)\ln(\alpha+0.07706)$$

$$-(y_{min}+0.07706)\ln(y_{min}+0.07706)$$

where $\alpha=y_{max}$ or 12.75, whichever is smaller, and $\beta=(\alpha-y_{min})$. For the portion of the interval $(y_{max}-y_{min})$ that is beyond 12.75 ft,

$$\int_{\gamma}^{y_{max}} f(y)\,dy=(y_{max}-\gamma)$$

where $\gamma=\gamma_{y_{min}}$ or 12.75, whichever is greater.

Propeller jet velocity (V_j'), where it passes over the pod and strut, is calculated at the apex of the pod curvature following methods described by Saunders.[4] In the tractor pod configuration tested here, the jet diameter (D_j') is calculated to be 16.85 ft at 22 ft abaft the propeller disk. So, out of an 8.73-ft mean strut height, 5.05 ft is in the hull wake and the rest in the propeller jet. Jet velocity (V_j') is 1.0635 times the advance velocity (V_A) averaged across the propeller disk.

Physical dimensions from the model-test configurations and resulting wake fractions and jet velocities used in predicting the model-test results are summarized in Tables 6 and 7. The computed results are compared to model-test results in Table 11 and a sample calculation is given in the Appendix.

Model Tests

A series of model experiments were conducted by Hydronautics Ship Model Basin to measure ship performance with pods. The test program was designed primarily to evaluate and compare effective horsepower (EHP) and shaft horsepower (SHP) requirements for tractor and pusher pod configurations. The diameter of the tested pods corresponds to that expected to be achieved with superconductive homopolar motors, which are being developed by David Taylor Naval Ship Research and Development Center (see Table 1). As many variables as possible were held constant to limit model-test costs, produce directly comparable results, and enhance the validity of the tests. The same hull, rudders, and propellers were used in all three configurations and the bilge keels and skeg were retained throughout the tests. The rudder was not integrated into the pod/strut body and the depth of

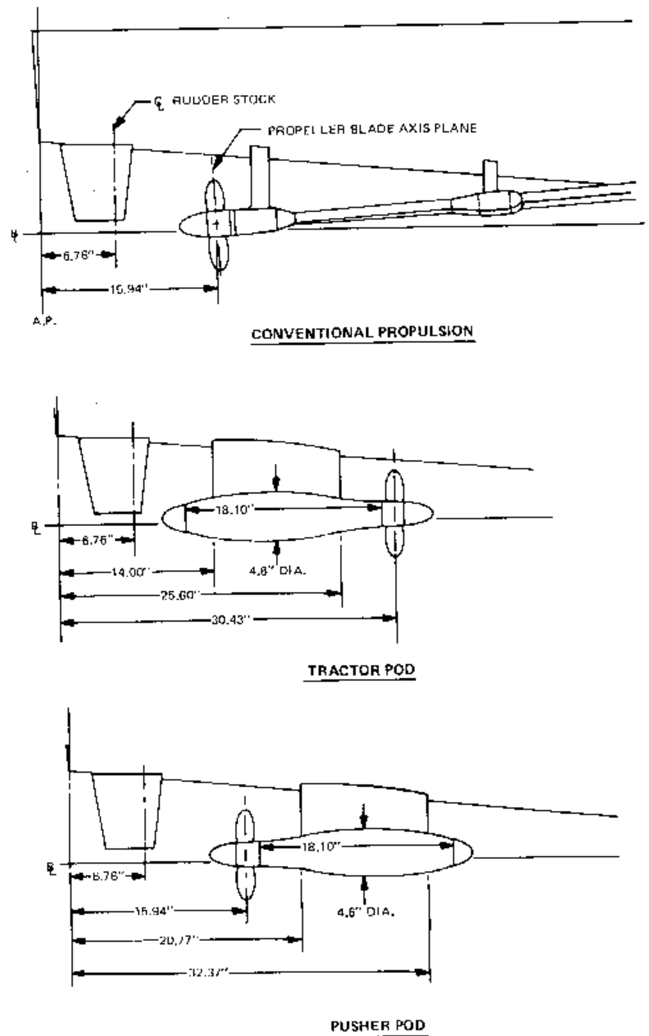

Fig. 3 Comparison of conventional and pod-strut appendages for model.

the propeller axis was held constant in all configurations. A DD-963 class hull configuration was used for the tests.

The DD-963 class model was constructed of fiberglass on a scale ratio of 24.84 (Table 8 lists the full scale ship and model particulars). The particulars were the same for all three configurations except for the wetted surface which changed as noted in Table 8.

The model was tested with twin rudders, skeg, bilge keels, sonar dome, and propulsion appendages. Figure 3 shows a sketch of the three configurations for the propulsion appendages.

For the two podded configurations, a single set of struts and pods was constructed in such a way as to allow it to be used for both the pusher and tractor configurations by rotating the pods on the struts and changing the fairwater. The rudders were installed at a 2-deg trailing-edge angle inboard for all tests. Figure 4 shows the model in the two podded configurations.

The propellers used for all the tests were aluminum-casted copies of the actual model design propellers for the DD-963 class ship. Figure 5 gives the characteristics of the model propellers.

The model tests were conducted in a basin 415-ft long, 24-ft wide and 12.5-ft deep. The EHP tests for all configurations were done over a full scale speed range of 12–34 knots. Two SHP tests were done for each configuration. Each test was a constant speed test with a variation of propeller-loading coefficients over a range corresponding to the EHP test range. One test was done at a scale speed of 24 knots and the other at 30 knots. For the standard propulsion appendages, both

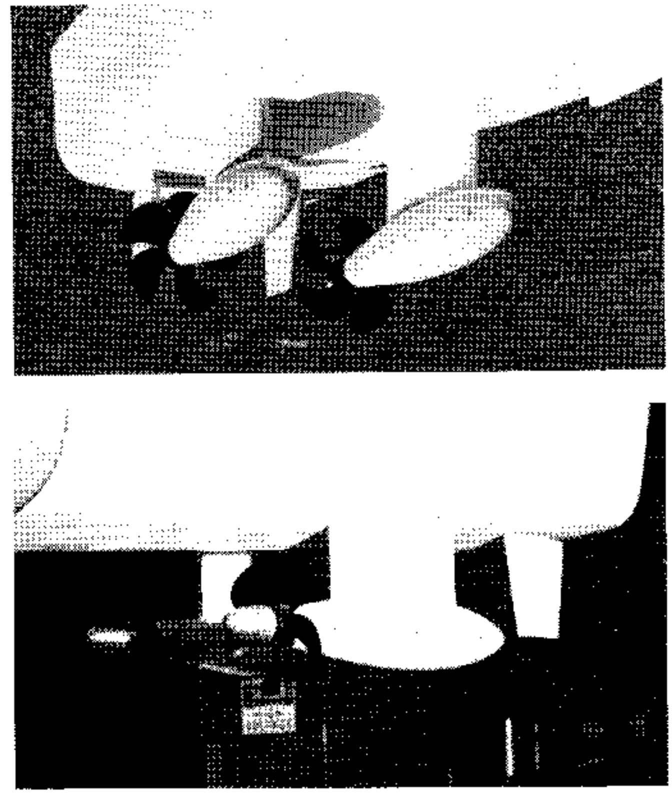

Fig. 4 Model with pusher (top) and tractor (bottom) pods.

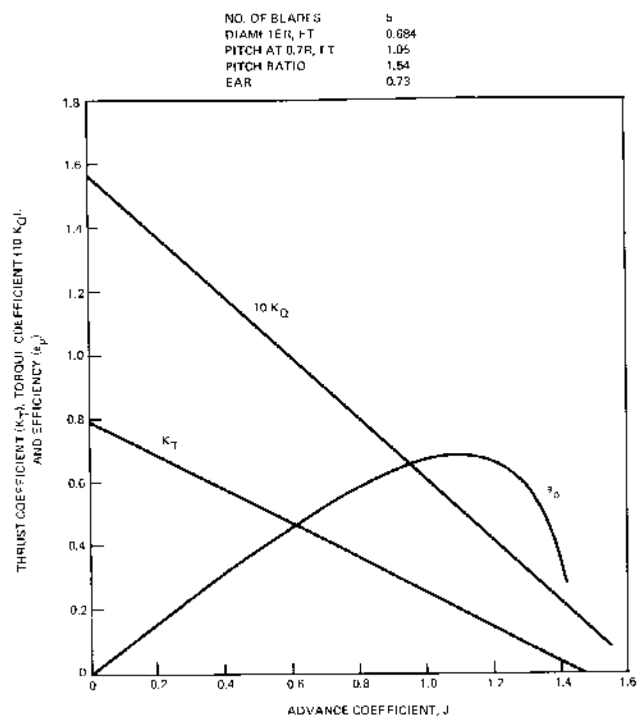

Fig. 5 Open-water characteristics of propellers used for testing.

Table 9 EHP of different propulsion configurations for DD-963 class destroyer

V, knots	No propulsion appendages	Conventional propulsion appendages	Tractor pods	Pusher pods
12	1885	2170	2072	2152
16	4415	5070	4891	4835
20	8339	9705	9908	9771
24	14,158	16,245	16,539	16,130
28	25,215	27,650	28,038	27,660
32	47,339	52,985	51,744	50,624

Table 10 Comparison of the SHP for the three model-test configurations

	Conventional propulsion appendages		Tractor pods		Pusher pods	
Speed, knots	24	30	24	30	24	30
e_p	0.659	0.659	0.659	0.659	0.659	0.658
e_h	0.959	0.956	0.962	0.935	0.930	0.932
e_{rr}	0.999	0.981	1.000	1.000	1.000	1.000
Propulsive coefficient	0.631	0.618	0.634	0.616	0.613	0.613
EHP	16245	39330	16539	39115	16130	37949
SHP	25745	63641	26087	63498	26313	61907
SHP/SHP conventional	1.000	1.000	1.013	0.998	1.022	0.973

Table 11 Comparison of computation and model-test results

Ship speed, knots	Propulsors	EHP for propulsors Model-test	EHP for propulsors Computation	δ[a] (EHP)	$\delta/B\times 100\%$ $B=$EHP for model test propulsors, %	$\delta/B\times 100\%$ $B=$EHP for model test ship, %
24	Twin tractor pods	2381	2183	−198	−8	−1
24	Twin pusher pods	1972	1681	−291	−15	−2
34	Twin tractor pods	3826	4209	+383	+10	+1
30	Twin pusher pods	2660	3232	+572	+22	+2

[a] δ = (Computation result)—(model-test result).

thrust and torque of both propellers were measured. For the podded propulsion tests, only torque for each propeller was measured.

The tests were accomplished using a yaw head pitot tube to determine the lines of flow at the stern in the region of the pod attachments. The tests were conducted at two speeds: 24 and 30 knots full scale. The probe was mounted at two locations, one corresponding to the center of the tractor pod strut and the other corresponding to the center of the pusher pod strut. Based on the results from the lines of flow tests, the pods were installed at a 2.5-deg trailing-edge angle inboard. Table 9 lists the EHP for all hull and appendage configurations tested.

Figure 5 shows the open water curves for the model propellers used in the tests. Table 10 lists values of SHP measured at 24 and 30 knot scale speeds for each configuration. Table 10 also compares the various efficiencies of the alternative propulsion systems and gives a merit figure for the different configurations in form of a ratio of SHP-to-SHP conventional. Although individual speed values show more or less variation from the conventional appendages, the average among speeds is such that the systems could be described effectively as having equivalent performance.

Comparison—Models and Computation

Appendage drag is a complex problem and difficult to predict closely. The differences between computed predictions and model-test results in this study are well within normal ranges of error and between 1 and 2% of the total ship drag. Table 11 lists effective horsepower requirements of twin pods and struts (excluding hull and other appendages) as determined by computation and model tests. When compared to the propulsor EHP requirement, the difference ranges from −15 to +22%; but when compared to the total ship EHP requirement, the difference ranges from −2 to +2%.

Table 10 compares the shaft horsepower requirements of the three configurations in the model tests. No significant differences in propulsion efficiency or appendage drag are found under the conditions of these tests (same hull and same non-propulsion appendages). Podded propulsors neither improve nor diminish propulsive performance if the hull size is not reduced and if the excess appendages are not removed. When the entire ship is designed to take full advantage of pods, the performance of podded propulsors is expected to be significantly better than the performance of conventional open shafts and multiple struts.

Conclusions

No significant hydrodynamic performance penalty is incurred by adding podded propulsion nacelles to a destroyer hull. The test results and model analysis indicate this, which is reassuring. The appendage drag of the shafting and struts matches well against the pod drag. The advantages of low noise, compactness, and producibility are all realized without a drag penalty; and it would now be valuable to conduct maneuvering tests for the pod/hull model. Analysis indicates that the turning radius of a podded destroyer increases without significant changes in rudder size and design, because of the fin effect of the pods.

A very important factor in the propulsion performance—the wave-making effects of the pods—has not been included in this hydrodynamic analysis. The distance of the pod centerline to the water surface is only about two times that of the pod diameter. Hence, the pods should influence the wave-making drag of the ship.

An effect similar to the "bulbous bow" is anticipated. This may explain why at very high speeds—say, 30-plus knots—the ship EHP requirement of podded propulsion is less than that of conventional propulsion. Theoretical and experimental studies concerning the wave-making effect of a podded system on a ship are recommended, so that optimal configuration and position of a podded system can be determined.

Appendix: Sample Calculation for Twin Pods and Struts at 24 Knots

Dimensions: $L_{pod}=52.15$ ft, $D_{pod}=9.5$ ft, $C_{strut}=24$ ft, $t_{strut}=3.6$ ft, $h_s=8.73$ ft.

Nacelle Drag:

$$Rn=\frac{V_jL}{\gamma}=\frac{(1.0060)(24)(1.689)(52.15)}{1.2791\times 10^{-5}}=1.6626\times 10^{8}$$

$$C_f=\frac{0.075}{[(\log_{10}Rn)-2]^2}=1.9381\times 10^{-3}$$

$$C_D=C_F[1+1.5(0.1822)^{1.5}+7(0.1822)^{3.0}]$$

$$=(1.1590)C_f=2.2463\times 10^{-3}$$

$$M=\sqrt{1+4(L/D)2}=\sqrt{1+4(52.15/9.5)2}=11.0244$$

$$S=(\pi D^2/3)[M+1/(M+1)]=1049.7401\text{ ft}^2$$

$$\text{drag} = C_D(\rho/2)SV_j^2$$
$$= (2.2463 \times 10^{-3})(1.9905/2)(1049.7401)$$
$$= [(1.0060)(24)(1.689)]^2 = 3903 \text{ lb for one pod}$$

Strut in Jet:

$$Rn = \frac{(1.0060)(24)(1.689)(24)}{1.2791 \times 10^{-5}} = 7.6515 \times 10^7$$

$$C_f = \frac{0.075}{[\log_{10} Rn - 2]^2} = 2.1665 \times 10^{-3}$$

$$C_D = 2C_f[1 + 2(0.1500) + 60(0.1500)^4]$$
$$= (2.6608)C_f = 5.7646 \times 10^{-3}$$

$$S = 2(D_j'/2 - D_{\text{pod}}/2)C = 2(3.6767)(24) = 176.4816 \text{ ft}^2$$

$$\text{drag} = C_D(\rho/2)SV_j^2$$
$$= 1684 \text{ lb for the portion of one strut in the jet}$$

Strut in Hull Wake:

$$Rn = \frac{(1-\omega)V_s L}{\gamma} = \frac{(0.6374)(24)(1.689)(24)}{1.2791 \times 10^{-5}} = 4.8480 \times 10^7$$

$$C_f = \frac{0.075}{[\log_{10} Rn - 2]^2} = 2.3201 \times 10^{-3}$$

$$C_D = 2C_f[1 + 2(0.1500) + 60(0.1500)^4]$$
$$= (2.6608)C_f = 6.1733 \times 10^{-3} = 242.5608 \text{ ft}^2$$

$$S = 2\left(h_s - \frac{D_j - D_{\text{pod}}}{2}\right)C = 2\left(8.73 - \frac{16.8533 - 9.5}{2}\right)(24)$$

$$\text{drag} = C_D(\rho/2)SV_A^2$$
$$= (6.1733 \times 10^{-3})(1.9905/2)(242.5608)$$
$$\times [(0.6374)(24)(1.689)]^2$$
$$= 995 \text{ lbs for the portion of one strut in the hull wake}$$

Strut-Hull Junction:

$$C_D = (0.20)[17(0.1500)^2 - 0.05] = 66.5000 \times 10^{-3}$$

$$\text{drag} = C_D(\rho/2)T^2 V_A^2$$
$$= (0.0665)(1.9905/2)(3.6)^2[(0.0803)(24)(1.689)]^2$$
$$= 9 \text{ lb for one strut-hull junction}$$

Strut-Pod Junction:

$$\text{drag} = C_D(\rho/2)T^2 V_j^2$$
$$= (0.0665)(1.9905/2)(3.6)^2[(1.0060)(24)(1.689)]^2$$
$$= 1426 \text{ lb for one strut-pod junction}$$

Pod-to-Pod Proximity:

$$s/t = 102/\pi D - 1 = 102/\pi(9.5) = 2.4177$$

$$C_D = (0.155)\exp\left[-\frac{(s/t) - (0.25)^{1.1}}{1.1}\right] = 0.0210$$

$$S = (\pi/4)D^2 = (\pi/4)(9.5)^2 = 70.8822$$

$$\text{drag} = C_D(\rho/2)SV_A^2$$
$$= (0.0210)(1.9905/2)(70.8822)[(0.9852)(24)(1.689)]^2$$
$$= 2363 \text{ lb for one pod}$$

Pod-to-Hull Proximity:

$$y/d = 8.73/9.5 = 0.9189$$

$$C_D = (0.0642)(y/d)^{5.7818} = (0.0642)(0.9189)^{5.7818} = 0.0394$$

$$S = (\pi/4)d^2 = (\pi/4)(9.5)^2 = 70.8822$$

$$\text{drag} = C_D(\rho/2)SV_A^2$$
$$= (0.0394)(1.9905/2)(70.8822)[(0.9852)(24)(1.689)]^2$$
$$= 4433 \text{ lb for one pod}$$

Total Twin-Pod/Strut Drag = (2)(14,813) = 29,626 lb

Effective Horsepower

$$= \frac{(\text{total drag}) \times V_A}{550} = \frac{(29{,}626)(24)(1.689)}{550} = 2183 \text{ hp}$$

References

[1] Rains, D.A., VanLandingham, D.J., and Doyle, T.J., "Podded Destroyer Propulsion," *Naval Engineers Journal*, Vol. 91, April 1979, pp. 120-130.

[2] Stewart, A.J., Springer, J.H., and Doyle, T.J., "Effectiveness of Superconductive Electric Drives," *Naval Engineers Journal*, Vol. 91, April 1979, pp. 109-119.

[3] Hoerner, S.F., *Fluid Dynamic Drag*, Hoerner Fluid Dynamics, Bricktown, N.J., 1965, Chaps. 8 and 13.

[4] Saunders, H.E., *Hydrodynamics in Ship Design*, Society of Naval Architects and Marine Engineers, New York, 1957, Vol. 1, p. 508 and Vol. II, pp. 342, 706.